College of Engineering

Society of Manufacturing Engineering of Iran

University of Tehran

3rd International Conference on Manufacturing Engineering
ICME2011, Tehran, Iran
27-29 December 2011

Design and Fabrication of an Out of Plane Micro-Inertial Sensor

A. M. Khodadadi Behtash[1], F. Barazandeh[1*] and N. Sayyaf[1]

[1] *Department of Mechanical Engineering, Amirkabir University of Technology, Tehran, Iran*

Abstract

The function of a micro accelerometer depends on several performance parameters such as resolution, sensitivity and noise level. This paper presents design and fabrication of an optimized micro-machined out of plane capacitive accelerometer. The accelerometer consists of a proof mass and four folded beams fabricated on a 100 μm thick single crystal silicon (SCS) substrate using high aspect ratio reactive ion etching (RIE) process. The optimization process is carried out by the use of non-dominated sorting genetic algorithm (NSGA-II) by considering performance requirements and manufacturing process limitations, such as mask printing resolution and minimum feasible feature size in RIE process. The optimization process will present a Pareto optimal front by a set of optimal designs. In order to achieve a design with maximum conformity with the read out circuit requirements, a trade off should be made between solutions. So the limits for the electrical circuit can be changed without any new optimization process.

Keywords**:** *MEMS sensor; Optimization; Pareto front; Performance parameter; Trade off*

1. Introduction

MEMS acceleration sensors are widely used in applications such as inertial navigation and guidance systems, seismology, micro-gravity measurements and crash detection for air-bags. The function of a micro accelerometer depends on several performance parameters such as resolution, sensitivity and noise level; thereby an optimum design requires a good tuning of these parameters which may have conflicting nature [1]. Optimization methods can be used to achieve an optimum design which satisfies all of the performance parameters in a suitable way. In many optimized accelerometers reported so far there are two approaches to reach an optimized design. In the first approach, the exploitation of a single performance factor as a fitness function is considered for the optimization procedure [2, 3]. In the second approach the aim is to optimize a primary objective function which is a combination of several secondary objective functions [4]. In these optimization methods each run of the optimization process results in an optimized design regarding to the performance requirements but any change in these requirements needs new run of optimization program.

The subject of this paper is to design and fabricate a MEMS acceleration sensor by considering fabrication and performance functions limitations. The optimization procedure is carried out by a Non-dominated sorting genetic algorithm (NSGA-II) [5] on three objective functions including: the ratio of mechanical noise to sensitivity, natural frequency and full range capacitance. Finally, the optimized design of the accelerometer is fabricated by the use of reactive ion etching (RIE) process.

2. Sensor Design

A schematic of the accelerometer is shown in Fig. 1. The accelerometer consists of an out of plane proof mass with folded type beams which are connected in four places to the supporting frame. This frame is bonded to the upper and lower caps with thermo compression bonding (TCB) method. Metalized plates on both sides of moving mass and caps, form variable capacitances to sense the external acceleration applied to the sensor. In order to satisfy fabrication resolution and to reduce the space required for the mechanical part, the overall size is considered to be less than 7×7 mm^2.

3. Theoretical modeling

As shown in Fig. 1, the four folded beams suspend the proof mass against the inertial force (due to acceleration). Besides the inertial force, the squeeze film damping effect is also present. The squeeze film effect is due to the trapped air between the proof mass and the stationary plates (upper and lower caps) [6]. In this section some of the important performance parameters which define the specifications of an accelerometer, will be introduced and formulated.

3.1 Natural Frequency

Natural frequency is one of the important parameters that can affect the dynamic behavior of an

*Corresponding author. Tel: +98 21 64543442, Fax: +98 21 66419736
E-mail address: fbarazandeh@aut.ac.ir

accelerometer. The first resonant mode of the designed accelerometer can be calculated as a function of total spring constant K, and the equivalent mass M, using spring-mass lumped parameter model:

$$f_n = \frac{1}{2\pi}\sqrt{\frac{K}{M}} \quad (1)$$

In Eq. (1), the total spring constant K, is the sum of three spring constants (Eq. (2)) including: K_{mech} as mechanical stiffness and K_{elec} as negative electrostatic stiffness [6].

$$K = K_{mech} + K_{elec} \quad (2)$$

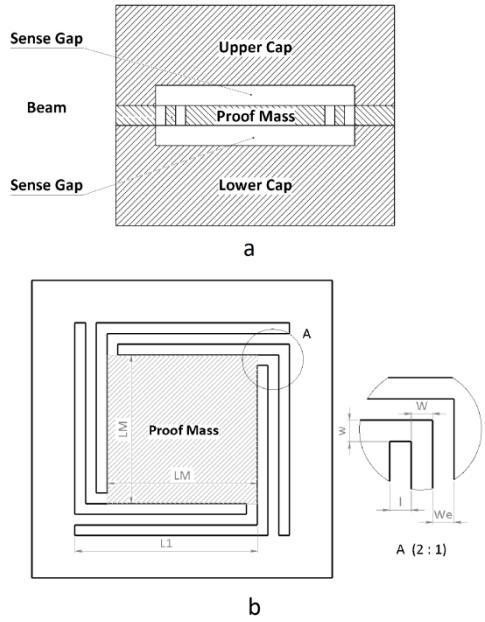

Fig. 1 Proposed micro-accelerometer a) the whole system b) proof mass dimensions

Mechanical stiffness is calculated by the Eq. (3), in which, E is the elastic modulus for silicon beam, W the width of the beam, t the thickness of the beam and L is the beam length.

$$K_{mech} = 4\frac{EWt^3}{L^3} \quad (3)$$

Also, the electrostatic stiffness can be calculated by the use of Eq. (4).

$$K_{elec} = -2\frac{C_0 V^2}{d_0^2} \quad (4)$$

Where C_0 is the initial capacitance between two parallel plates, V the rms excitation voltage applied to the plates by readout circuit and d_0 is the initial gap between two capacitance plates. The equivalent mass contributed in Eq. (1) can be expressed as Eq. (5):

$$M = \left[\left(\frac{52}{35}L + 200\times10^{-6}\right)W + L_M^2\right]t\rho \quad (5)$$

In this equation, ρ is the density of the silicon. In order to consider the mass of the beam, it is assumed that the total mass of the beam is lumped on the beam's tip.

3.2 Squeeze film damping

In a MEMS structure especially with an oscillating part, package gas pressure can profoundly affect the dynamic behavior of the system. This effect originates from damping pressure acting on the moving plate. If one of the plates oscillates in y direction (i.e.: in the direction perpendicular to the cap faces) due to an applied acceleration a_{in}, the following equation of motion can be written to represent the plate oscillation:

$$M\times\ddot{y} + b\times\dot{y} + K\times y = M\times a_{in} \quad (6)$$

Where b is the damping coefficient of the air trapped in the package and can be expressed by the Eq. (7):

$$b = \frac{96\mu L_M^4}{\pi^4 d_0^3} \quad (7)$$

3.3 Brownian noise

The total noise of a micro accelerometer originates from two different sources: mechanical noise and electric readout circuit noise. The total noise for a MEMS acceleration sensor is calculated in Eq. (8) [3].

$$Noise_{total} = \sqrt{Noise_{\text{mech}}^2 + Noise_{\text{elec}}^2} \quad (8)$$

Mechanical noise is an intrinsic noise due to damping and is called Brownian motion noise which results from the random collision of air molecules with the proof mass [7]. The Brownian noise depends on the surrounding gas temperature T, damping coefficient b (Eq. (7)) and the equivalent mass contributing in the oscillation M (Eq. (5)). The acceleration noise resulted from Brownian noise is introduced in Eq. (9).

$$Noise_{mech} = \sqrt{\frac{4K_B Tb}{M}}\ \left[\frac{m}{s^2}/\sqrt{Hz}\right] \quad (9)$$

In this equation K_B is the Boltzman constant.

3.4 Mechanical Sensitivity

The sensitivity is the ratio of an output value to input. In this section the mechanical sensitivity will be regarded as the total sensor sensitivity. Considering Eq. (6), mechanical sensitivity of the accelerometer can be defined as Eq. (10).

$$Mechanical_{sens} = \frac{1}{\sqrt{(\omega_n^2 - \omega^2) + \left(\frac{b}{M}\omega\right)^2}} \quad (10)$$

Where, $\omega_n = 2\pi f_n$ and ω is defined to be the radial frequency of the input acceleration.

3.5 Capacitive pick-off

Changing proof mass position causes capacitance changes in both sides of the moving mass, the readout circuit will detect the acceleration by the difference of capacitances in both sides, and this value can be expressed as the Eq. (11):

$$\Delta C_a = C_1 - C_2 = \frac{2\varepsilon_0 A y^2}{d_0^2 - y^2} \quad (11)$$

Where ΔC_a is the full range capacitance change in the applied acceleration a_{in} and ε_0 is the permittivity of the dielectric (in this case air).

4. Optimization procedure

In order to achieve a suitable design for fabrication process, an optimization process is carried out. The aim of this process is to obtain a design which possesses optimum values for each of the performance parameters introduced in the previous sections and also satisfies the initial values required for read out circuit.

4.1 Non Dominated Genetic Algorithm (NSGA-II)

Over the recent decades, numbers of multi-objective evolutionary algorithms (MOEAs) are introduced, Multi-Objective Genetic Algorithm (MOGA) by Fonseca and Fleming, Non-dominated Sorting Genetic Algorithm (NSGA) by Srinivas and Deb, Niched Pareto Genetic Algorithm (NPGA) by Horn, Pareto-Archived Evolution Strategy (PAES) by Knowles and Strength Pareto Evolutionary Algorithm (SPEA) by Zitzler and Thiele are some of these proposed methods [8]. These kinds of algorithms are desirable to solve multi-objective optimization problems because of capability to handle a set of solutions in a single run of the algorithm simultaneously in compare with single objective methods. NSGA-II, proposed by Deb et al [5], is one of the most efficient and well known multi-objective evolutionary algorithms which use non-dominated sorting and crowding distance techniques to rank and select population fronts. Steps used in this algorithm are shown in Fig. 2.

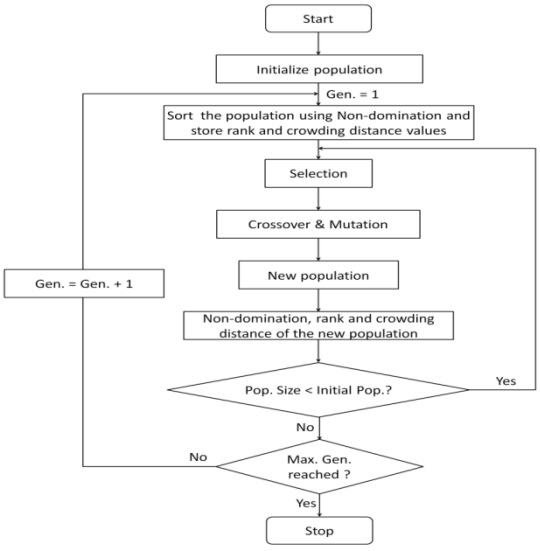

Fig. 2 Flowchart of NSGA-II algorithm

Detailed principle of this algorithm considering Fig. 2 is as follows: In the first step the population is initialized based on the problem range and constraints, then individuals are sorted to different levels called front levels. Each front is assigned a non-domination number or a rank number starting from 1 as the top and non-dominated one, this procedure continues until the last level reaches. In addition to ranking, a parameter called crowding distance is adopted to calculate the local density of individuals. This parameter shows an approximation of the perimeter of the Cuboid formed by the nearest neighbors as the vertices. In other words the crowding distance of the *ith* solution in its front is the average length of the sides of the Cuboid formed by *(i-1)th* and *(i+1)th* solutions (Fig. 3); After the individuals are sorted based on non-domination and with crowding distance assigned, the selection is carried out using the binary tournament selection, where two solutions are picked from the population and the better solution is chosen. Since there is no need to employ a penalty parameter, this process is very attractive.

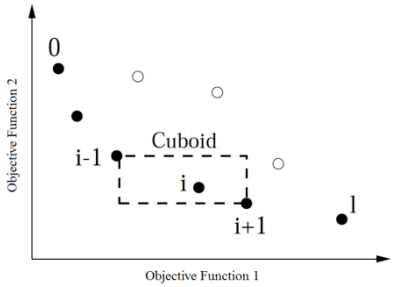

Fig. 3 Crowding distance calculation

After these steps, by using crossover and mutation operators (as in classical GA) offspring population Q_i is formed. Thereafter, new population R_i is formed by the combination of a random parent population P_i of size N and also offspring population of the same size (i.e. $R_i=Q_i+P_i$), so the size of new population is 2N.

After all above, again the new population is sorted and assigned a rank number according to non-domination. Consequently, a new population P_{i+1} will be obtained by removing the solutions overflowing N. Repeating these processes, a group of optimum solutions will be achieved. These are called Pareto optimal fronts and the decision maker can select each of them as a solution for the problem. In this paper the population size of 100 and 1000 generations is used. The crossover and mutation probability rates are set on 0.75 and 0.05 respectively.

5. Objective Functions and Limit Values

In order to reach an optimized design, three different functions are used as objective function:

1) Minimization of the ratio between mechanical noise to sensitivity.

$$f = \sqrt{\frac{4K_B Tb}{M}\left[(\omega_n^2 - \omega^2) + \left(\frac{bs}{M}\omega\right)^2\right]} \quad (12)$$

2) Maximization of natural frequency.
3) Maximization of full range capacitance change.
Each of these functions is taken as a distinct objective function in multi-objective procedure and a set of non-dominated solutions has been obtained using NSGA-II.

Limitations in fabrication processes such as lithography and mask printing resolution accentuates some of design variables to be limited to achieve a suitable design for manufacturing processes. Table 1 shows the ranges for the proof mass length (L_M), beam length (L), beam width (W) and initial gap (d_0) as independent variables.

6. Results

Optimization procedure is carried out by the use of multi objective genetic algorithm (NSGA-II) and linear inequalities presented in Table 1. The aim of the optimization is to minimize the ratio presented in the Eq. (12), to maximize the natural frequency and full range capacitance change in 20g acceleration range. In a multi-objective optimization problem generally there is not a single optimum solution that minimizes all of the objective functions simultaneously and several trade-off solutions (Pareto fronts) are usually selected as the optimum results [5]. The 3D and 2D plots of the optimum fronts for this method are shown in Fig. 4, 5 and 6. In the first step in order to find optimum designs for the fabrication process, extremum designs for each objective are selected as initial designs. As shown in figure 4, there are two extremum points for the diagram which will result in extremum values for each of the objective functions. The values for independent variables and also the objective functions are presented in table 2.

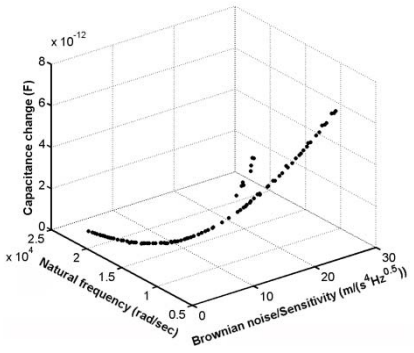

Fig. 4 Pareto optimal fronts for Brownian noise / sensitivity, capacitance change and natural frequency

The natural frequency for the first design is the biggest one among the other designs but this design has the smallest full range capacitance change in 20g acceleration range, so it cannot result in a good resolution for the measured acceleration during the operation of the sensor, moreover the designed values for initial capacitance of the first design may not satisfy the readout circuit limitations (9pF < C_0 < 17pF). Although the second design has the biggest full range capacitance change amongst all other designs, both of the initial capacitance and the full range capacitance change for this design are not in the acceptable range for the readout circuit. However, these designs can be used in other fabrication processes by different readout circuits.

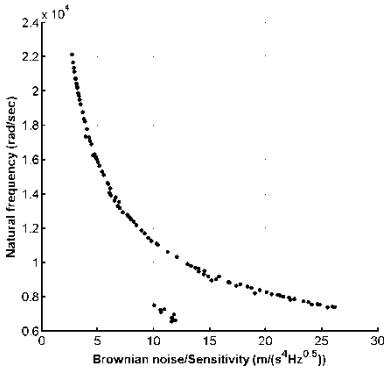

Fig. 5 Pareto optimal fronts for Brownian noise / sensitivity and natural frequency

Table 1 Optimization limits for independent variables

Variables	Limits	
	Lower	Upper
Proof mass length (mm)	3.3	4.9
Beam length (mm)	3.5	5.9
Beam width (μm)	50	100
Initial gap (μm)	15	20

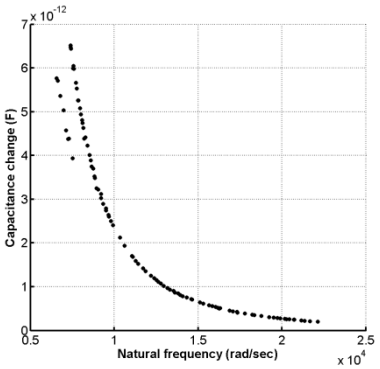

Fig. 6 Pareto optimal fronts for natural frequency and capacitance change

In order to satisfy the readout circuit limitations and also select a design within the optimized range, a trade off should be made between designs, so the read out circuit limitations are added into the diagram shown in Fig. 7. According to this figure, designs inside the borders of the rectangle are acceptable for the fabrication process with the desired hybrid readout circuit. Achieving the highest resolution for this sensor requires a high initial capacitance in addition to the high

capacitance change. In this way a trade-off design shown in Table 2 is selected for the final fabrication process. The overall full range capacitance change for this design (trade off) is 3.89 pF which is near the maximum value desired for this change according to read out circuit. Moreover the value for the initial capacitance is in the middle of the range allotted for this value.

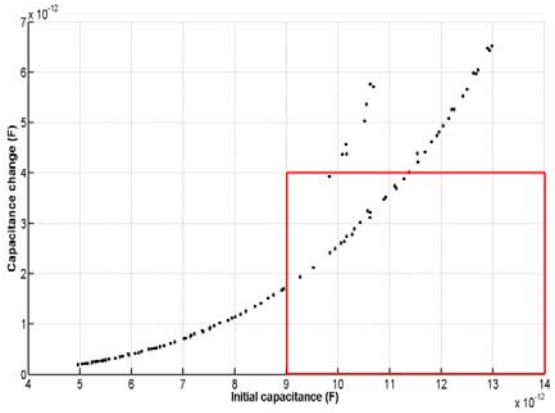

Fig. 7 Pareto optimal fronts for initial capacitance and capacitance change considering read out circuit limit (rectangular area)

The fabrication process needs three different lithography masks. The first mask is used for the proof mass and beam patterning on Cr layer for hard mask formation and the two other masks are designed for fixed capacitance plate formation and metal layer deposition, respectively.

The proof mass fabrication starts with a standard chemical mechanical polishing (CMP) process of an N-type (100) silicon wafer. By this process, the wafer is thinned to 100 µm. After this step, a 0.2 µm Cr layer deposited on the wafer surface and then the pattern of the suspension beams and the area of the proof-mass and supporting frame are defined on Cr layer by photolithography process. In the next step of the fabrication process, in order to achieve the proof mass and also folded beams with sharp and vertical side walls, RIE process is employed [9].

In the final step, after removing the Cr layer by standard processes, electrodes are formed by the use of Au sputtering process on both sides of the wafer. Fig. 8 depicts the view of fabricated proof mass prior to the bonding process.

The wafer used for caps is 500 µm thick N-type one. The whole process for this part except the final RIE step is the same as in the proof mass fabrication. The difference is in the RIE process depth and the final lift off metallization step for metalized plate fabrication.

The bonding process is carried out for about 2 hours in 360°C under the pressure of 80 MPa. After the dicing process, in order to prepare wire connections between the mechanical element and readout circuit, the bonded substrates are attached to the supporting substrate.

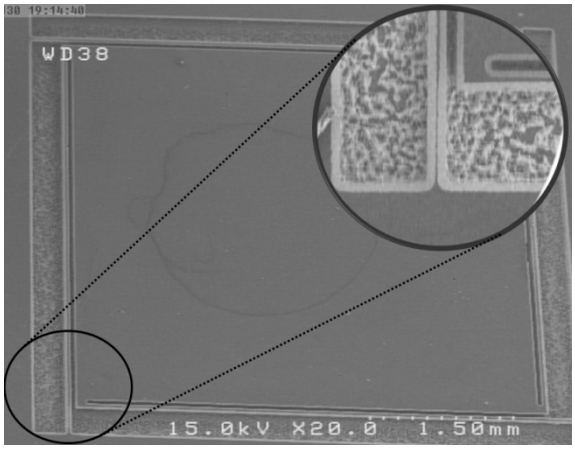

Fig. 8 SEM picture of fabricated MEMS element

7. Conclusion

A capacitive out of plane micro accelerometer is designed and implemented. In order to design a sensor with optimum performance parameters, geometrical dimensions of the sensor are optimized using non dominated sorting genetic algorithm (NSGA-II). The constraints used in this process as variable boundaries are provided by the fabrication and readout circuit limitations. NSGA-II algorithm shows a good convergence to the optimum results according to the applied limitations. The multi-objective genetic algorithm (NSGA-II) provides a set of optimum results where the selection between results is to the designer. Extremum results selected for the design show little conformity with the capacitive limitations of the read out circuit, so a trade off selection between designs in

Table 2 Optimization results for extremum values of functions and trade off design

		Variables					Sensor specifications		
	Optimization criteria	Length of mass, L_M (µm)	Beam length, L (µm)	Beam width, W (µm)	Initial gap, d_0 (µm)	Brownian noise / Sensitivity ($m/(s^4Hz^{0.5})$)	Initial capacitance, C_0 (pF)	Capacitance change, ΔC_{20g} (pF)	Natural frequency (rad/sec)
1	Brownian Noise / Sensitivity	3319.6	3529.1	85.7	20.0	2.71	4.90	0.21	22137.36
2	Capacitance change	4701.1	5309.3	64.3	15.1	26.21	8.21	6.52	7406.35
3	Trade-off	4486.8	5034.8	67.6	16.0	18.36	11.30	3.89	8604.50

the acceptable range would be a big advantage of the multi objective approach. Considering this optimization method, a trade off optimum design is selected according to mechanical, electrical and fabrication process limits. If the limits for the electrical circuit changed, other designs can be suggested from the diagram. This method facilitates the designing procedure and new dimensions can be obtained without any new optimization.

References

[1] N. Yazdi, F. Ayazi, K. Najafi, "Micromachined inertial sensors", *Proceedings of the IEEE*, vol. 86, No. 8, pp. 1640-1659, 1998.

[2] J. Chae, H. Kulah, K. Najafi, "A CMOS compatible high aspect ratio silicon-on-glass in-plane micro-accelerometer", *J. Micromech. Microeng*, Vol. 15, pp. 336–345, 2005.

[3] P. Monajemi, F. Ayazi, "Design Optimization and Implementation of a Microgravity Capacitive HARPSS Accelerometer", *IEEE Sensors Journal*, vol. 6, No. 1, pp. 39-46, 2006.

[4] J.K. Coultate, CHJ. Fox, S. McWilliam, AR. Malvern, "Application of optimal and robust design methods to a MEMS accelerometer", *Sensors and Actuators A*, vol. 142, pp. 88-96, 2008.

[5] K. Deb, A. Pratap, S. Agarwal, T. Meyarivan, "A Fast and Elitist Multiobjective Genetic Algorithm: NSGA-II", *IEEE Transactions on evolutionary computation*, vol.6, No.2, pp. 182-197, 2002.

[6] M. Bao, H. Yang, "Squeeze film air damping in MEMS", *Sensors and Actuators A*, vol. 136, pp. 3-27, 2007.

[7] SD. Senturia, "Microsystem design", Kluwer Academic Publishers, New York, 2001.

[8] A. Konak, DW. Coit, AE. Smith, "Multi-objective optimization using genetic algorithms: A tutorial". *Reliability Engineering and System Safety*, vol. 91, pp. 992-1007, 2006.

[9] IW. Rangelow, H. Loschner, "Reactive ion etching for microelectrical mechanical system fabrication" *Journal of Vacuum Science & Technology B: Microelectronics and Nanometer Structures*, vol. 13, No. 6, pp. 2394-2399, 1995.